

Neurobiology

Glycinergic Innervation of Motoneurons Is Deficient in Amyotrophic Lateral Sclerosis Mice

A Quantitative Confocal Analysis

Qing Chang* and Lee J. Martin*†

From the Department of Pathology,* Division of Neuropathology, and the Department of Neuroscience,† Johns Hopkins University School of Medicine, Maryland

Altered motoneuron excitability is involved in amyotrophic lateral sclerosis pathobiology. To test the hypothesis that inhibitory interneuron innervation of spinal motoneurons is abnormal in an amyotrophic lateral sclerosis mouse model, we measured GABAergic, glycinergic, and cholinergic immunoreactive terminals on spinal motoneurons in mice expressing a mutant form of human superoxide dismutase-1 with a Gly93→Ala substitution (G93A-SOD1) and in controls at different ages. Glutamic acid decarboxylase, glycine transporter-2, and choline acetyltransferase were used as markers for GABAergic, glycinergic, and cholinergic terminals, respectively. Triple immunofluorescent labeling of boutons contacting motoneurons was visualized by confocal microscopy and analyzed quantitatively. Glycine transporter-2-bouton density on lateral motoneurons was decreased significantly in G93A-SOD1 mice compared with controls. This reduction was absent at 6 weeks of age but present in asymptomatic 8-week-old mice and worsened with disease progression from 12 to 14 weeks of age. Motoneurons lost most glycinergic innervation by 16 weeks of age (end-stage) when there was a significant decrease in the numbers of motoneurons and choline acetyltransferase-positive boutons. No significant differences in glutamic acid decarboxylase-bouton densities were found in G93A-SOD1 mice. Reduction of glycinergic innervation preceded mitochondrial swelling and vacuolization. Calbindin-positive Renshaw cell number was decreased significantly at 12 weeks of age in G93A-SOD1 mice. Thus, either the selective loss of inhibitory glycinergic regulation of motoneuron function or glycinergic interneuron degeneration contributes to motoneuron de-

generation in amyotrophic lateral sclerosis. (Am J Pathol 2009, 174:574–585; DOI: 10.2353/ajpath.2009.080557)

Amyotrophic lateral sclerosis (ALS) is a rapidly evolving adult onset neurological disease characterized by a progressive loss of motoneurons.^{1,2} About 10% of ALS cases are familial ALS with inheritance patterns, and 90% are sporadic ALS with no known genetic component. Autosomal dominant mutations in the *Cu/Zn superoxide dismutase-1 (SOD1, ALS1)* gene occur in ~20% of familial ALS cases.³ Transgenic mice overexpressing the human mutated *SOD1* gene with a glycine/alanine substitution at codon 93 (G93A) develop a fatal motoneuron disease resembling ALS in humans.⁴

Many theories have been communicated that implicate perturbations in axonal transport, protein integrity, mitochondria, antioxidant status, and inflammation in the mechanisms of ALS pathogenesis.^{5,6} Considerable data supported the contributions of glutamate-mediated excitotoxicity in ALS.^{7–9} Alpha-amino-3-hydroxy-5-methyl-4-isoxazolepropionic acid receptors in spinal motoneurons were altered in human ALS^{10,11} and G93A-SOD1 mice.^{12–14} Electrophysiological studies of ALS patients indicated widespread signs of motoneuron hyperexcitability.¹⁵ Hyperexcitability of motoneurons was also observed in spinal cord slices¹⁶ and dissociated embryonic cell cultures from G93A-SOD1 mice.¹⁷

The hyperexcitability theory emphasizes mostly the contribution of excessive synaptic excitation, while the possibility of insufficient synaptic inhibition has been largely ignored. Spinal cord slice cultures from embryonic G93A-SOD1 mice showed an imbalance between

Supported by a grant from NIH-NS034100.

Accepted for publication October 16, 2008.

Supplemental material for this article can be found on <http://ajp.amjpathol.org>.

Address reprint requests to Lee J. Martin, Ph.D., Department of Pathology, Johns Hopkins University School of Medicine, 720 Rutland Avenue, 558 Ross Building, Baltimore, Maryland 21205. E-mail: martinl@jhmi.edu.

excitatory and inhibitory innervation.¹⁸ Spinal cord motoneurons receive extensive glycinergic and GABAergic innervations that regulate motoneuron excitability through various mechanisms.¹⁹ Abnormal gamma aminobutyric acid (GABA) and glycine levels were observed in serum or autopsy tissues of ALS patients.^{20,21} In human ALS autopsy spinal cord, binding sites for the inhibitory neurotransmitter glycine have been reported to be reduced in anterior horn.^{22,23} It therefore seems possible that inhibitory neural systems are disrupted as part of the pathogenesis in ALS. In fact, riluzole, the only drug approved by the Food and Drug Administration for the treatment of ALS, directly interacts with GABA(A) and glycine receptors^{24,25} in addition to its antiglutamatergic action.²⁶

In this study, we examined glycinergic and GABAergic innervations of spinal motoneurons in G93A-SOD1 mice using quantitative confocal analysis. We demonstrated that abnormalities in inhibitory interneuron innervations of spinal motoneurons emerge early in the course of disease before structural evidence for motoneuron degeneration.

Materials and Methods

Animals

Adult male transgenic mice expressing human mutant *SOD1* gene driven by the human *SOD1* promoter⁴ were studied. A mouse line (B6SJL-TgN [SOD1-G93A] 1Gur, G1H) with a high copy number of mutant alleles (~20 copies) and a rapid disease onset was used. The mice were studied through the entire course of the disease from asymptomatic stage to end-stage disease at 6, 8, 10, 12, 14, and 16 weeks of age. The group size for each data set was 3 to 5 mice. Controls were non-transgenic littermates of the mutants. The institutional Animal Care and Use Committee approved the animal protocols.

Tissue Preparation

Mice were overdosed with sodium pentobarbital (50 mg/kg) and subsequently perfused transcardially with ice-cold 100 mmol/L phosphate buffer-saline (pH 7.4) followed by 4% paraformaldehyde. All mice were perfused under identical conditions by the same individual. Spinal cords were postfixed in paraformaldehyde for 3 hours, and then were cryoprotected in 20% glycerol overnight. Transverse serial sections (40 μm -thick) through lumbar spinal cord were cut on a sliding microtome (American Optical Corporation, New York, NY) and stored individually in 96-well plates in cyroprotectant buffer (1% polyvinylpyrrolidone, 40% ethylene glycol, and 0.1 mol/L potassium acetate, pH 6.5) at -20°C until used for immunocytochemistry.

Triple Fluorescence Immunocytochemistry

Free-floating sections were rinsed in Tris buffer (TBS, pH 7.4), permeabilized with 0.4% Triton X-100, blocked with 10% donkey serum, and then incubated in a cocktail of primary antibodies diluted in TBS containing 2% donkey

serum and 0.1% Triton X-100 for 48 hours at 4°C . The primary antibodies used in different combinations were: mouse anti-glutamic acid decarboxylase 67 (GAD67; monoclonal, 1:10000; Chemicon, Temecula, CA); guinea pig anti-glycine transporter-2 (GlyT2; polyclonal, 1:10000; Chemicon); goat anti-choline acetyltransferase (ChAT; polyclonal, 1:200; Chemicon); rabbit anti-manganese-containing SOD (MnSOD, SOD2; polyclonal, 1:400; Assay Designs, Ann Arbor, MI); rabbit anti-growth associated protein-43 (GAP43; polyclonal, 1:1000; Chemicon); rabbit anti-synaptophysin (polyclonal, 1:1000; Dako Denmark A/S, Glostrup, Denmark). After four washes with TBS, sections were incubated for 2 hours at room temperature in a mixture of species-specific secondary antibodies (all raised in donkey) conjugated to Alexa Fluor 488, Alexa Fluor 594, or Alexa Fluor 647 (Invitrogen Corporation, Carlsbad, CA). Sections were washed again, and mounted using Prolong anti-fade medium (Invitrogen).

Confocal Microscopy and Quantification

Spinal cord sections were imaged using a 100 \times oil immersion objective (1.3 numerical aperture lens) mounted on a Zeiss LSM 510 confocal microscope. All sections were imaged under identical conditions and analyzed using identical parameters. ChAT immunoreactivity was used as a marker to identify motoneurons²⁷ in lateral and medial pools. Motoneurons are large cells (mean diameter $>20 \mu\text{m}$ for α -motoneurons) likely to be truncated within 40 μm sections. Only motoneurons with visible nuclei and nucleolus were selected. Immunolabeled presynaptic boutons were examined for apposition to ChAT-labeled large neurons. Boutons were considered to be in apposition only if there was no visible space between the bouton and the cell membrane in any optical section.

Measurements of immunopositive boutons were performed using NIH Image J software. Each confocal image obtained in triple staining experiments was split into three channels and thresholded in black and white binary images. Automatic intensity thresholding and particle sizes of above 0.18 μm^2 for GAD- and GlyT2-immunostaining or 0.22 μm^2 for ChAT-immunostaining were chosen for defining boutons. Standardized bouton number was determined by dividing the number of boutons contacting a motoneuron by its perimeter, which was measured using Image J software. The single optical section image for each neuron was measured at the level of the nucleolus. Lateral and medial motoneuron pools were analyzed separately. To evaluate regional selectivity, GlyT2-immunoreactivity was analyzed specifically in lamina II of dorsal horn. Confocal images were obtained at 100 \times from randomly selected regions within lamina II identified by location. Two different confocal images from each lumbar spinal cord section and two sections from each mouse were quantified.

To better resolve the density of boutons on the entire motoneuron cell bodies, we examined the bouton density throughout one half of the cell body in the lateral motoneurons. Total numbers of boutons per neuron divided by 2 were counted across the z-series optical sections

(0.7 μm separation). This was accomplished by starting at the first optical section containing a given neuron and counting the number of new boutons touching the cell surface to the last optical section at the middle of the soma. The "middle" was determined by scanning back and forth through the optical sections containing intact nuclei and nucleolus several times. The locations of labeled boutons in a single optical section were compared with labeled boutons in adjacent sections to avoid double counting of the same boutons. The bouton densities were calculated by dividing the total number of boutons by its surface area, which was determined by Image J software. Eight to ten motoneurons per spinal cord and two to three lumbar spinal cord sections per animal were quantified.

For colocalization analysis, images were imported into Image J software where regions of interest were outlined, and regions outside regions of interest were cleared using "segmenting assistant" plug-in. Each channel was then subjected to background subtraction, and analyzed by "colocalization threshold" plug-in (zero-zero pixels was excluded in threshold calculation). The thresholds for each channel were then calculated and pixels below this value were ignored for colocalization quantification. This method avoids the investigator bias in the thresholds setting. A pixel was defined as having colocalization when the intensities of both labels were above their respective thresholds. Using this method Pearson's correlation coefficient for pixels where either channel was below their respective threshold was 0.002 ± 0.005 ($n = 58$), and Pearson's correlation coefficient for pixels where both channels were above their respective threshold was 0.862 ± 0.005 ($n = 58$), indicating the thresholds had been set appropriately. Colocalization of synaptophysin with GlyT2-, GAD- or ChAT-immunoreactivity was given as the colocalization coefficients M1 and M2. These coefficients are proportional to the number of colocalizing pixels in either channel (channel 1 or channel 2) of the composite image, relative to the total number of pixels above threshold in that channel. Colocalization coefficient using threshold takes into account the number of pixels with colocalization as well as the intensities of the two labels in each pixel. The number of pixels (divided by perimeter) that have both channel 1 and channel 2 intensities above the threshold (ie, the number of colocalized pixels) was used to quantify the colocalization of GAP43-with GlyT2- or GAD-immunoreactivity.

Results are presented as mean \pm SEM. Statistical significance was determined by Student's *t*-test. The level of significance was set of $P < 0.05$.

Calbindin Immunohistochemistry

Lumbar spinal cord sections from G93A-SOD1 and control mice were used to localize calbindin D28k as a marker for Renshaw cells.²⁸⁻³¹ Calbindin was localized using a standard immunoperoxidase method with a mouse monoclonal antibody to calbindin (1:10,000; Sigma, St. Louis, MO) and visualized with diaminobenzidine (Sigma) as chromogen. Cell counts were made

by viewing sections under a 40 \times lens mounted on a Nikon microscope. Renshaw cells were identified by their location and characteristic morphology as described previously.^{31,32}

Results

The G93A-SOD1 transgenic mice with a high copy number of mutant allele first show signs of spasticity at about 10 weeks of age, and then unilateral or bilateral hindlimb paresis at around 11 to 12 weeks of age; the disease then progresses to end-stage when the mice are quadriplegic at around 16 weeks of age.^{4,33}

In this transgenic line of mutant SOD1 mice, the morphology and number of motoneurons changes dramatically over the time course examined by confocal microscopy. At 6 and 8 weeks of age, the cytoplasm of ChAT-positive motoneurons appeared uniform with no or minimal cytoplasmic vacuolization, and the size and shape of motoneuron perikarya appeared normal (Figure 1A). No significant differences in the number of large

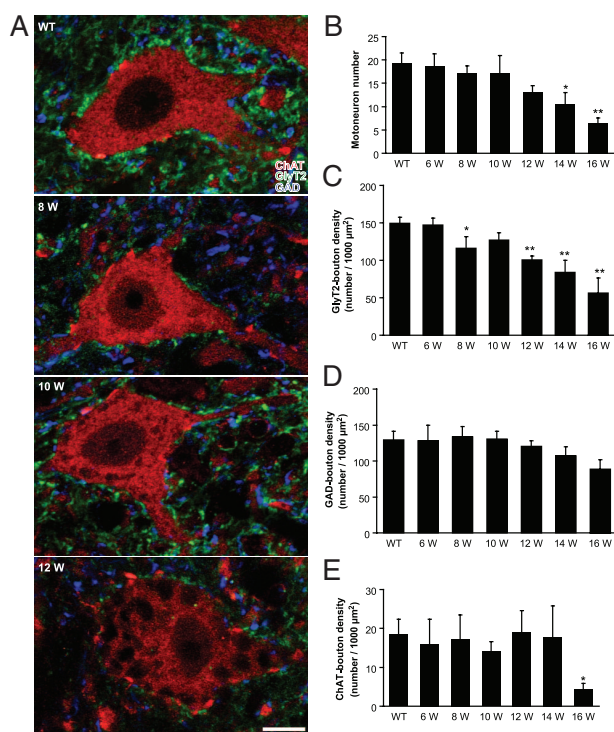


Figure 1. A: Confocal images of motoneurons in lumbar spinal cord sections triple labeled with GlyT2 (green), GAD (blue), and ChAT (red) in wild-type mice (WT) and G93A-SOD1 mice at 8, 10, and 12 weeks (W) of age. Each panel corresponds to a single optical section. Scale bar = 10 μm . **B-E:** Quantitative analysis of the GlyT2- (**C**), GAD- (**D**), and ChAT- (**E**) immunopositive boutons contacting the ChAT-immunopositive motoneurons and the number of motoneurons (**B**) from wild-type and G93A-SOD1 mice at 6, 8, 10, 12, 14, and 16 weeks of age. A significant decrease in the density of GlyT2-boutons was observed at asymptomatic 8-week-old G93A-SOD1 mice (**C**), before the decrease of the number of motoneurons (**B**). Motoneurons lost the majority of GlyT2-boutons at 16 weeks of age (**C**). No significant difference was observed in the density of GAD-boutons at all ages (**D**). Significant differences in the density of ChAT-boutons were not found until end-stage (16 weeks) in G93A-SOD1 mice (**E**). Data represent the mean \pm SEM (* $P < 0.05$, ** $P < 0.01$, Student's *t*-test). $n = 3$ to 5 mice per group. Eight to ten motoneurons per spinal cord and two to three lumbar spinal cord sections per animal were quantified.

ChAT-positive motoneurons were observed in 8-week-old G93A-SOD1 mice compared with controls (Figure 1B). At 10 weeks of age, some motoneuron cell bodies and proximal dendrites showed cytoplasmic vacuoles (Figure 1A). Swollen, degenerating axons with segmental enlargements were also seen in the ventral horn neuropil and white matter. At 12 weeks of age, cytoplasmic vacuoles in motoneurons were more apparent and more motoneurons possessed vacuoles (Figure 1A). At this time, subsets of motoneurons and axons were severely swollen, but the decrease in the number of motoneurons was not significant (Figure 1B). The number of motoneurons was decreased significantly at 14 weeks of age (Figure 1B; $P < 0.05$). At 16 weeks of age, when the disease developed to end-stage, the number of motoneurons was reduced further (Figure 1B; $P < 0.01$) and the residual motoneurons tended to be smaller than that the typical α -motoneurons.

GlyT2-Bouton Densities on Motoneurons Decrease in G93A-SOD1 Mice

Glycinergic synapses on lumbar spinal motoneurons were identified by GlyT2-immunoreactivity.^{34–36} Numerous densely-packed, flattened GlyT2-immunopositive boutons (averaged $1 \mu\text{m}^2$ in size; Figure 1A, green) were closely apposed to the soma and proximal dendrites of ChAT-positive large motoneurons. Bouton density was analyzed to determine changes in glycinergic innervation. In this analysis, the number of boutons was expressed as a ratio of total surface area. We quantified GlyT2-positive boutons through the surface of half of the motoneuron (providing they had visible nucleus and nucleolus) cell bodies (z-stack) from both wild-type and G93A-SOD1 mice. All motoneurons analyzed in wild-type mice were contacted by GlyT2-positive boutons. No significant differences in the distribution and density of boutons between the soma and proximal dendrites of motoneurons, or differences in GlyT2-bouton densities between different ages of wild-type mice were observed (data not shown).

At 6 weeks of age, G93A-SOD1 mouse motoneurons had GlyT2-bouton densities similar to wild-type mice (Figure 1C). However, GlyT2-bouton densities were significantly lower in asymptomatic 8-week-old G93A-SOD1 mice than in controls (Figure 1C; $P < 0.05$). About 20% of GlyT2-boutons were lost on G93A-SOD1 mouse motoneurons. Individual variation was observed between 8-week-old G93A-SOD1 mice (Figure 1C, error bar), mirroring the individual variation in the onset of disease. No obvious changes were observed in the size and shape of remaining GlyT2-boutons on G93A-SOD1 mouse motoneurons. Unexpectedly, the density of GlyT2-boutons showed a slight recovery at 10 weeks of age with respect to the 8-week-old G93A-SOD1 mice (Figure 1C). At 12 weeks of age, when the mice were paretic, GlyT2-bouton densities were decreased significantly. Fewer individual variations were observed at this age compared with 8-week-old mice. The loss in GlyT2-boutons was more pronounced at 14 weeks of

age. At 16 weeks of age, when the disease developed to end-stage, motoneurons lost the majority of GlyT2-boutons (Figure 1C).

Compensatory Up-Regulation of Glycinergic Innervation of Motoneurons in 10-Week-Old G93A-SOD1 Mice

The number of GlyT2-positive boutons slightly recovered at 10 weeks of age compared with 8-week-old G93A-SOD1 mice (Figure 1C). Considering the possibility of compensatory recovery, we triple labeled the spinal cord with GlyT2-, ChAT-, and GAP43-antibodies. GAP43 is a neurite outgrowth marker.^{37–40} GAP43-immunoreactivity was observed as bouton-like swellings in apposition to motoneurons (Figure 2A). Colocalization of GlyT2- and GAP43-immunoreactivity was detected in wild-type mice (Figure 2A). The colocalization coefficients of GlyT2 with GAP43 ($M1$; calculated as $M1 = \text{pixels}_{\text{Ch1, colocal}} / \text{pixels}_{\text{Ch1, total}}$, where Ch1 is GlyT2) was 0.127 ± 0.023 ($n = 3$). At 6 and 8 weeks of age, the average number of GAP43/GlyT2 colocalized pixels was not significantly different compared with control (Figure 2B). GAP43/GlyT2 colocalized pixel number significantly increased in 10-week-old G93A-SOD1 mice (Figure 2B; $P < 0.05$). The colocalization coefficients of GlyT2 with GAP43 also increased to 0.182 ± 0.026 ($n = 3$). Because GAP43 marks neurite sprouting,^{40,41} the increase of its

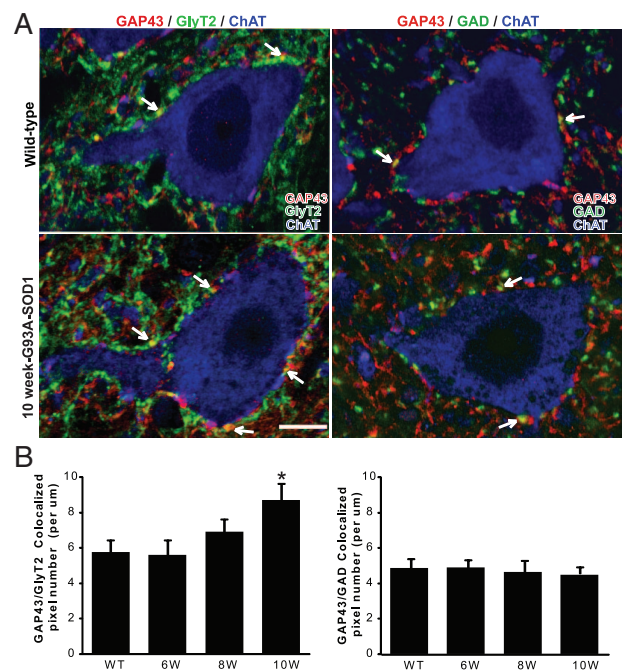


Figure 2. A: Confocal images of lumbar spinal motoneurons showing colocalization (yellow, **arrows**) of GlyT2 (**left**, green) or GAD (**right**, green) with GAP43 (red) in apposition to ChAT-positive neurons (blue) in wild-type and 10-week-old G93A-SOD1 mice. Scale bar = $10 \mu\text{m}$. **B:** Quantitative analysis of colocalization. Graphics show the average numbers of GAP43/GlyT2 (**left**) or GAP43/GAD (**right**) colocalized pixels representing the axonal growth in wild-type and G93A-SOD1 mice at 6, 8, and 10 weeks (W) of age. Analysis of GAP43/GlyT2 colocalization revealed statistically significant increases in the area of immunofluorescent colocalization in 10-week-old G93A-SOD1 mice compared with control. Data represent the mean \pm SEM (* $P < 0.05$, Student's *t*-test). $n = 3$ mice per group.

colocalization with GlyT2-immunoreactivity indicates sprouting of glycinergic terminals in 10-week-old G93A-SOD1 mice.

To test the specificity of glycinergic terminal sprouting on motoneurons, we also studied the colocalization of GAD- and GAP43-immunoreactivity. The colocalization coefficients of GAD with GAP43 (M1; calculated as $M1 = \text{pixels}_{\text{Ch1, colod}} / \text{pixels}_{\text{Ch1, total}}$, where Ch1 is GAD) was 0.115 ± 0.019 ($n = 3$). No significant differences were found in GAP43/GAD colocalized pixel numbers at 6, 8, and 10 weeks of age compared with controls (Figure 2B).

GABAergic Innervation of Motoneurons Is Maintained in G93A-SOD1 Mice

GABAergic synapses contacting motoneurons were identified using an antibody to GAD67.⁴² The same large ChAT-positive motoneurons that were contacted by GlyT2-boutons were also contacted by round or oval GAD-immunopositive boutons that averaged $1 \mu\text{m}^2$ in size (Figure 1A, blue). No significant differences in the density of GAD-boutons on motoneuron soma were observed in G93A-SOD1 mice at any ages (Figure 1D). The size, shape, and distribution of GAD-boutons on motoneurons were not different in G93A-SOD1 mice compared with controls. At end-stage disease (16 weeks), the absolute number of GAD-positive boutons on individual motoneurons decreased because the residual motoneurons are relatively small at these ages, but the density of GAD-boutons remained unchanged.

Cholinergic Innervation of Motoneurons in G93A-SOD1 Mice Is Preserved at Early Stages of Disease

ChAT-positive motoneurons were also contacted by large (average size $2.2 \mu\text{m}^2$) ChAT-positive boutons, resembling the C-boutons.^{43,44} These boutons were distributed sparsely on soma and proximal dendrites of most motoneurons (Figure 1A, bright red). At 6, 8, 10, 12, and 14 weeks of age, no significant differences were found in the densities of ChAT-positive boutons between G93A-SOD1 and control groups (Figure 1E). Large individual variations were observed between individual mice in the same group (Figure 1E, error bar). A significant difference in the density of ChAT-boutons was found at end-stage disease (16 weeks) in G93A-SOD1 mice (Figure 1E, $P < 0.05$).

GlyT2 and GAD Colocalize with Synaptophysin on Motoneurons

To confirm that GlyT2- and GAD-immunoreactive structures are synaptic boutons, we triple labeled spinal cord sections with the neurotransmitter markers and synaptophysin, a ubiquitous synaptic vesicle marker.⁴⁵ Figure 3 illustrates the colocalization of GlyT2- and/or GAD-immunoreactivity with synaptophysin immunoreactivity closely

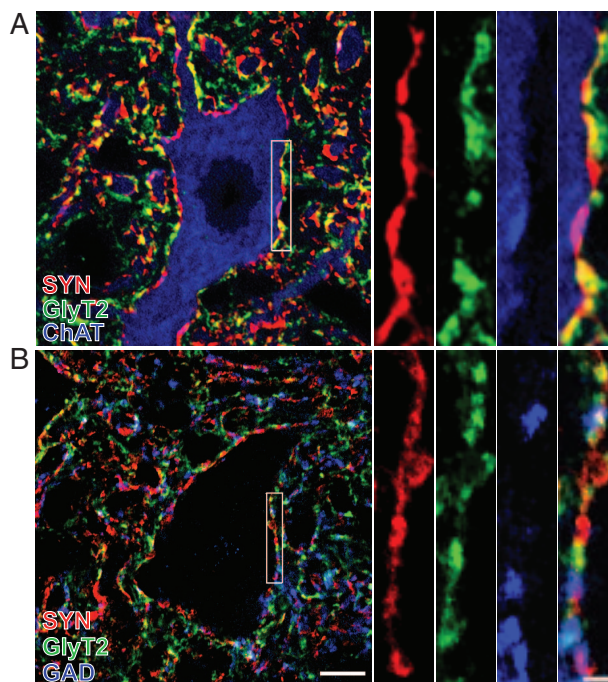


Figure 3. Optical sections of lumbar motoneurons illustrating GlyT2- (green), GAD- (**B**; blue), and ChAT- (**A**; blue) positive boutons colocalized with synaptophysin (SYN; red) immunoreactive presynaptic terminals. **A:** Colocalization (yellow) of GlyT2 and synaptophysin, and colocalization (pink) of ChAT and synaptophysin around the soma and proximal dendrites of ChAT-positive motoneurons. **B:** Colocalization (yellow) of GlyT2 and synaptophysin, and colocalization (pink) of GAD and synaptophysin around the putative motoneurons. Three-way colocalization (white) of GlyT2-, GAD-, and synaptophysin immunoreactivity was also observed. Scale bar = $10 \mu\text{m}$. The area delineated by white rectangular is shown of higher magnification at **right**. Scale bar = $2 \mu\text{m}$.

apposed to ChAT-positive neurons. Both GlyT2- and GAD- immunoreactivities had substantial colocalization with synaptophysin, though, as expected, structures other than synaptic boutons were also labeled (Figure 3A). The colocalization coefficients of GlyT2 or GAD with synaptophysin (M1; calculated as $M1 = \text{pixels}_{\text{Ch1, colod}} / \text{pixels}_{\text{Ch1, total}}$, where Ch1 is GlyT2 or GAD) were 0.707 ± 0.017 ($n = 10$ motoneurons) and 0.751 ± 0.028 ($n = 10$ motoneurons), respectively. Colocalization of GlyT2- with GAD-immunoreactivity was also observed, and the colocalization coefficient of GlyT2 with GAD was 0.313 ± 0.042 (M1; calculated as $M1 = \text{pixels}_{\text{Ch1, colod}} / \text{pixels}_{\text{Ch1, total}}$, where Ch1 is GlyT2; $n = 10$ motoneurons). Three-way colocalization of GlyT2, GAD and synaptophysin was detected (Figure 3B, white).

The colocalization coefficients of synaptophysin with GlyT2 or GAD (M2; calculated as $M2 = \text{pixels}_{\text{Ch2, colod}} / \text{pixels}_{\text{Ch2, total}}$, where Ch2 is synaptophysin) were calculated to determine the proportion of GlyT2- or GAD-boutons versus total presynaptic terminals, ie, synaptophysin immunoreactivity. The colocalization coefficients of synaptophysin with GlyT2 was 0.605 ± 0.046 ($n = 10$ motoneurons), and the colocalization coefficients of synaptophysin with GAD was 0.432 ± 0.041 ($n = 10$ motoneurons).

Unbiased Quantification of All Surviving Motoneurons

The above analytical strategy used on z-stack confocal images is a method that identified all immunoreactive boutons in contact with the entire surface of motoneuron cell bodies. However, it was not an unbiased sampling method because at least one half of the motoneuron cell body needed to be contained within the z-stack to obtain accurate bouton counts, thus limiting random selection to those neurons that meet this criteria. The size and number of motoneurons also change with disease progression in G93A-SOD1 mice,³³ so it is difficult to find appropriate criteria for motoneuron sampling. To solve this problem, all motoneurons on one side of the 40 μm -thick spinal cord sections in both wild-type and G93A-SOD1 mice were analyzed in single optical sections. The average size of motoneurons gradually increased from 10 weeks of age and reached maximum at 12 weeks in G93A-SOD1 mice, indicating swelling of motoneuron cell bodies (Figure 4A). At 14 weeks of age, the average size of motoneurons decreased compare to 12 weeks (Figure 4A), suggesting dissolution of some swollen motoneurons. Motoneurons were divided into two groups based on their Feret's diameters (determined by Image J software): 20–30 μm group (mid-size) and >30 μm group (large-size). We excluded the ChAT-positive neurons with diameters <20 μm that may be γ -motoneurons. The increase of motoneuron average sizes at 12 weeks of age was due to decreased mid-size motoneurons and slightly increased large-size (swollen) motoneurons (Figure 4B). The number of GlyT2-boutons contacting motoneurons in the large-size group tended to be slightly higher (but not significant) than in the mid-size motoneuron group in wild-type mice (Figure 4C). At 8 weeks of age, a reduction in the number of GlyT2-boutons was detected in both mid-size and large-size motoneuron groups in G93A-SOD1 mice (Figure 4C). A slight recovery of glycinergic innervation was observed in large-size motoneuron group at 10 weeks of age, accompanied by a slight increase in the number of motoneurons in the large-size category, which indicate swelling of motoneuron soma. Progressive loss of GlyT2-boutons was observed over time in G93A-SOD1 mice in both mid-size and large-size motoneurons (Figure 4C). No significant changes in the number of GAD- and ChAT-boutons were observed in G93A-SOD1 mice (Figure 4, D and E).

The number of GlyT2-positive boutons contacting the small (diameter <20 μm), ChAT-positive, putative γ -motoneurons was relatively few (~30% of the number of GlyT2-boutons contacting α -motoneurons), and no significant changes in the number of GlyT2-positive boutons contacting the presumable γ -motoneurons were observed in G93A-SOD1 mice compared with controls (data not shown).

The above analysis focused on the lateral motoneuron pool that primarily innervates distal muscles.⁴⁶ To determine whether the loss of glycinergic boutons is selective for the lateral motoneuron pool, the medial motoneuron

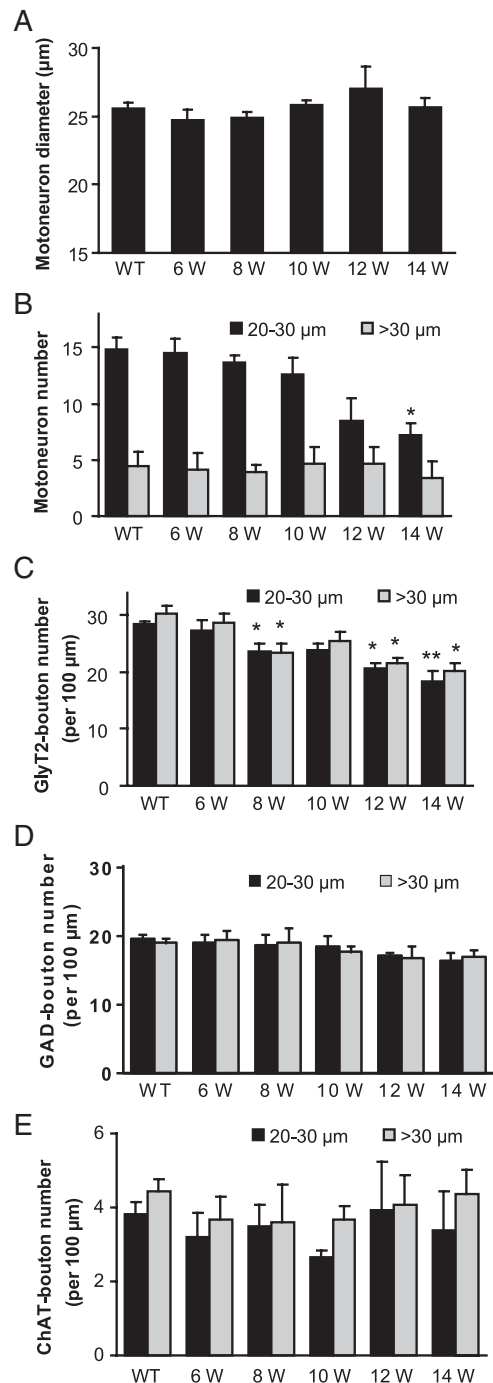


Figure 4. Unbiased quantification of all surviving lateral pool motoneurons from single spinal cord optical sections of wild-type mice (WT) and G93A-SOD1 mice at 6, 8, 10, 12, and 14 weeks (W) of age. The average size of motoneurons gradually increased from 10 weeks of age, reached maximum at 12 weeks, and started to decrease at 14 weeks in G93A-SOD1 mice (A). Motoneurons were divided into two groups based on their Feret's diameters: 20 to 30 μm group and >30 μm group, and the number of motoneurons in wild-type and G93A-SOD1 mice at different ages was shown in (B). The number of GlyT2- (C), GAD- (D), and ChAT- (E) immunopositive boutons contacting all surviving lateral motoneurons was also shown. Data represent the mean \pm SEM (* P < 0.05, ** P < 0.01, Student's t -test). n = 3 to 5 mice per group.

pool that innervates proximal muscles⁴⁶ was also analyzed. The medial pool of motoneurons has lower levels of glycinergic innervations compared with lateral pool motoneurons (Figure 4C, Figure 5A), and no significant de-

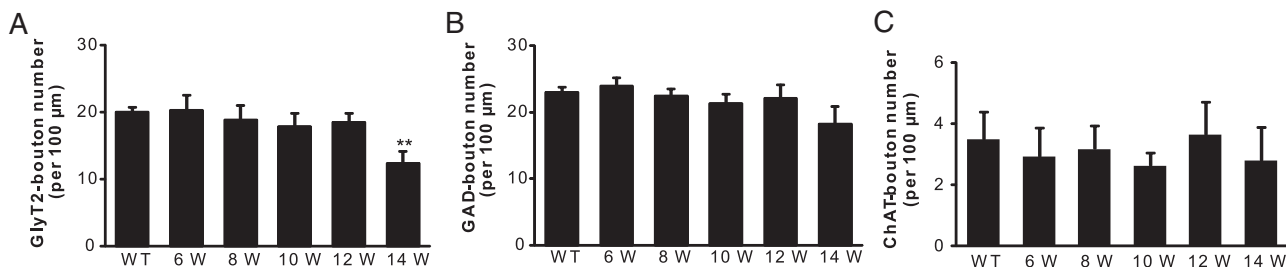


Figure 5. Quantification of GlyT2- (A), GAD- (B), and ChAT- (C) immunopositive boutons contacting all medial pool motoneurons from single spinal cord optical sections of wild-type mice (WT) and G93A-SOD1 mice at 6, 8, 10, 12, and 14 weeks (W) of age. No significant decrease in GlyT2-bouton number on medial motoneurons was observed until 14 weeks of age in G93A-SOD1 mice (A). Data represent the mean \pm SEM (** $P < 0.01$, Student's *t*-test). $n = 3$ to 5 mice per group.

crease in GlyT2-bouton number on medial motoneurons was observed until 14 weeks of age (Figure 5A). No significant differences in either GAD- or ChAT-bouton number on medial pool motoneuron soma were observed in G93A-SOD1 mice at 6, 8, 10, 12, and 14 weeks of ages (Figure 5, B and C).

The glycinergic innervations on lamina II cells in dorsal horn of spinal cord were analyzed to further investigate if the early changes in glycinergic innervations are a more widespread phenomenon rather than being specific for lateral motoneurons. No significant changes were observed in glycinergic innervations of lamina II cells in 8-week-G93A-SOD1 mice compared with controls (Supplemental Figure S1 available at <http://ajp.amjpathol.org>).

Reduction of Glycinergic Innervation Precedes Motoneuron Vacuolization and Mitochondrial Swelling

One of the first pathological abnormalities seen in high-expressing G93A-SOD1 mice is cytoplasmic vacuolization in motoneurons.^{33,47–49} This cytoplasmic microvacuolation has been attributed to swelling of mitochondria.^{33,50–52} An antibody to MnSOD that localizes in the mitochondrial matrix⁵³ was used to identify mitochondria in motoneurons. In wild-type mice, small, discrete, particulate-like or filament-like MnSOD-immunopositive mitochondria within cytoplasm were observed in ChAT-positive motoneurons (Figure 6, first row) and in some other cells in spinal cord. No obvious differences in MnSOD-immunoreactivity were observed in any of the 8-week-old G93A-SOD1 mice studied compared with control (Figure 6, second row). At 10 weeks of age, mitochondrial MnSOD-immunoreactivity became more prominent. For some mitochondria, their shape and size changed. In the cell bodies and proximal dendrites of some motoneurons and in dendrites within the neuropil, the vacuoles overlapped with large swollen MnSOD-positive mitochondria (Figure 6, third row). With many cytoplasmic vacuoles the overlap was only partial because MnSOD localizes to the mitochondrial matrix, but there is also swelling of the intermembrane space.⁴⁸ In some motoneurons, swollen mitochondria aggregated around the nucleus (data not shown). Mitochondrial swelling was relatively selective for motoneurons at early stages of disease because it was not apparent in other types of cells

including dorsal horn neurons and ChAT-positive interneurons in 10-week-old G93A-SOD1 mice. The onset of mitochondria swelling was not simultaneous in individual spinal motoneurons and not present in all mitochondria within a motoneuron. The mitochondrial swelling in some α -motoneurons and γ -motoneurons was very late in onset. No visible changes in MnSOD-immunoreactivity were observed in swollen ChAT-positive axons at 10 weeks of age. Fulminant mitochondrial swelling was observed in G93A-SOD1 mice at 12 weeks of age (Figure 6, last row).

Renshaw Cells Are Lost in G93A-SOD1 Mice

A specific class of glycinergic interneuron is called the Renshaw cell,^{54–56} which was identified as calbindin-

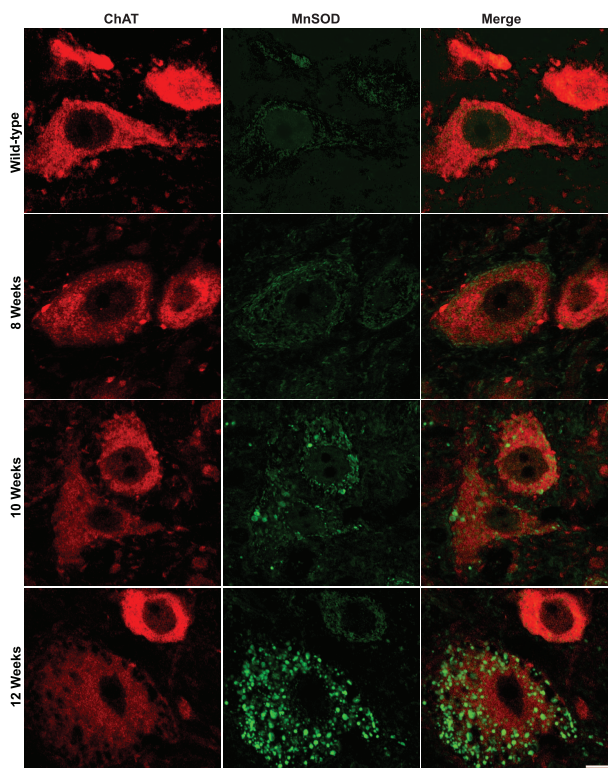


Figure 6. Representative images showing MnSOD labeling (green) within ChAT- (red) positive neurons in wild-type and G93A-SOD1 mice at 8, 10, and 12 weeks of age. No obvious MnSOD-positive mitochondrial swelling was observed until 10 weeks of age in G93A-SOD1 mice. Scale bar = 10 μ m.

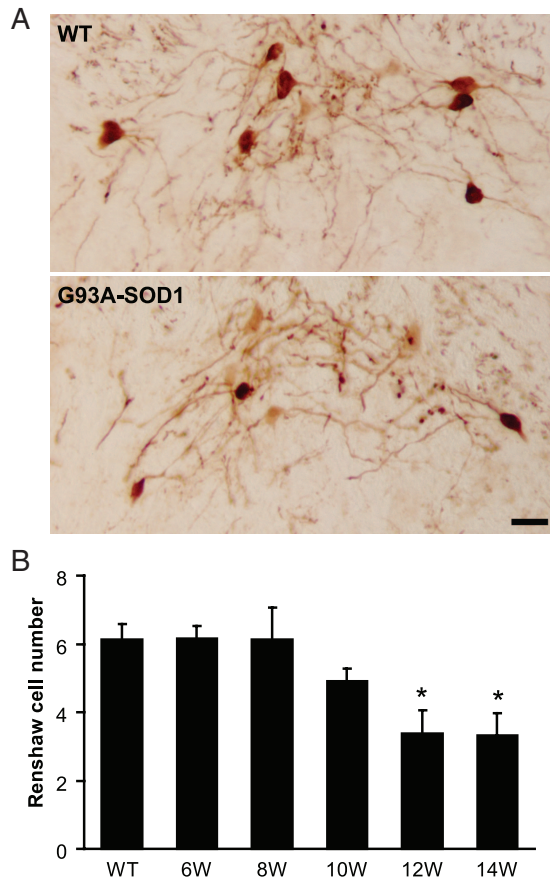


Figure 7. A: Immunocytochemistry shows calbindin-immunopositive Renshaw cells in the ventral horn of spinal cord sections from wild-type and G93A-SOD1 mice. Scale bar = 20 μ m. **B:** Quantitative analysis of Renshaw cell number from wild-type and G93A-SOD1 mice at 6, 8, 10, 12, and 14 weeks (W) of age. Data represent the mean \pm SEM (* P < 0.05, Student's *t*-test). n = 3 to 5 mice per group. Two to three lumbar spinal cord sections per animal were quantified.

immunoreactive neurons located in the ventral portion of lamina VII, medial to the motoneuron column.^{28–31,57} A distinct population of small (14 to 20 μ m in average diameter) and strongly immunolabeled calbindin-positive neurons was observed in spinal cord from wild-type mice (Figure 7A). The number of Renshaw cells was lower in 10-week-old G93A-SOD1 mice compared with control (Figure 7B). A significant decrease in the number of Renshaw cells was observed at 12 and 14 weeks of age in G93A-SOD1 mice (Figure 7B; P < 0.05). The loss of Renshaw cells preceded the reduction of motoneurons in G93A-SOD1 mice, which was not significantly decreased until 14 weeks of age (Figure 1B).

Discussion

The major finding of this study is that G93A-SOD1 mice have a reduction in glycinergic innervation on motoneurons at presymptomatic disease, which precedes major structural pathology in motoneuron cell bodies and proximal dendrites. This early glycinergic denervation is specific for lateral motoneurons. We interpret this finding as an early loss of inhibitory synaptic control of motoneurons

that could permit excitotoxic dysfunction in motoneurons in ALS.

We performed a novel quantitative confocal microscopy study of inhibitory innervations of spinal motoneurons in ALS mice. In our study, motoneurons were identified by ChAT-immunopositivity that was not lost completely until the end-stage of motoneuron degeneration, when the cell is in a severely necrotic-like state.³³ Thus ChAT is a reliable marker for motoneurons because it is maintained throughout the entire disease duration. Glycinergic and GABAergic synaptic terminals on motoneurons were detected with antibodies to GlyT2 and GAD67. GlyT2 is expressed in glycinergic boutons in mammals, where it is presumed to function in the presynaptic reuptake of transmitter at glycinergic synapses, making it an excellent marker for glycinergic neurons.^{35,36,58–62} In contrast to GlyT2, GlyT1 is an astroglial glycine transporter.^{60,61} Although immunoreactivity against the neuronal GlyT2 isoform is a reliable marker for glycinergic neurons,³⁴ GlyT2 antibody labels primarily axon terminals³⁵ and thus does not allow visualization of the cell bodies of glycinergic neurons for counting. Two forms of GAD, GAD65, and GAD67, responsible for synthesis of the inhibitory transmitter GABA, have been identified in vertebrates and mark GABAergic neurons.^{63–65} We chose GAD67 to study because this isoform is the major one found in boutons on spinal motoneurons.⁴² GAD antibodies also fail in the strong detection of GABAergic neuronal cell bodies, but yield excellent terminal labeling. We decided to analyze glycinergic and GABAergic boutons on motoneuron cell bodies because most of inhibitory innervations localized on the soma and proximal dendrites of motoneurons, while excitatory boutons located more distal on dendrites.¹⁹ We confirmed the terminal localizations of GlyT2 and GAD by their colocalization with synaptophysin.

We discovered that spinal motoneurons in G93A-SOD1 mice develop an early robust deficit in glycinergic innervation before light microscopic evidence of structural pathology. The deficit was not present at 6 weeks of age, indicating that the onset of GlyT2-bouton reduction occurs between 6 and 8 weeks of age, and thus is not developmentally pre-existing. It is possible that the reduction of GlyT2-immunoreactivity represents the loss of the glycine transporter-2 protein, but not the presynaptic terminals. Ultrastructural and functional study of the early axonal degeneration is therefore required as is a better understanding of whether glycinergic bouton loss is related to alternations in motoneuron glycine receptors.

In two recent studies, Zang et al and Schutz examined the presynaptic innervations of motoneurons in ALS mice.^{66,67} Neither of the studies was done using confocal microscopy, but both used the same transgenic line of G93A-SOD1 mice used here. Zang et al described a loss of synaptophysin-positive boutons on lumbar motoneurons of mice by 12 weeks of age.⁶⁶ Schutz described a loss in vesicular inhibitory amino acid transporter-immunoreactivity in motoneuron field in 110-day-old SOD1 mice.⁶⁷ However, the anti-vesicular inhibitory amino acid transporter did not detect the neurochemical nature of the inhibitory neurotransmitters, and no quantitative

analysis was conducted in their study. Synaptophysin was observed to be reduced in the anterior horn in post-mortem tissue of ALS patients.⁶⁸⁻⁷³ We believe that our finding is new and significant because the decrease of GlyT2-boutons possibly reflects an early degeneration of glycinergic synaptic terminals and the interneurons themselves, which occurs before the degeneration of motoneurons.³³ This abnormality could have significance with regard to the synaptic physiology of motoneurons.

Another interesting observation seen here is that the injured neurons appear to attempt compensation and recovery at 10 weeks of age as evidenced by the sprouting of glycinergic axons identified by their colocalization with GAP43. This is in consistent with a previous report that GAP43 expression on the surface of anterior horn cells was increased in postmortem tissue of ALS patients.⁷⁴ The recovery of glycinergic innervation was more obvious in large-size motoneuron group, which is likely to include a number of swollen, degenerating motoneurons, further support the idea that there maybe plastic alterations or a compensatory mechanism of the glycinergic axonal terminals located on the degenerating motoneurons.

The early loss of glycinergic innervations of lateral motoneurons is not a general, non-specific change in spinal cord of ALS mice. This conclusion is supported by two observations. First, glycinergic innervation of medial motoneurons was not decreased until near end-stage disease. Second, glycinergic innervation of dorsal horn lamina II cells was not compromised in ALS mice.

The loss of glycinergic innervation of motoneurons is neurotransmitter-selective because their GABAergic innervation is surprisingly maintained. In living patients with ALS, electrophysiological data revealed impaired intracortical inhibition.^{75,76} Positron emission tomography (PET) studies showed that binding of the benzodiazepine GABA(A) ligand flumazenil was reduced in the motor cortex of ALS patients.^{77,78} *In situ* hybridization histochemistry studies also indicated that GABA(A)-receptor mRNA expression was reduced in postmortem cortical samples of ALS patients,^{79,80} but unchanged in spinal cord of G93A-SOD1 mice.⁸¹ Our results are consistent with the observation that GABAergic innervations of lower motoneurons were unchanged. We found about 30% colocalization of GlyT2- with GAD-immunoreactivity, and it is possible that the glycinergic terminals that were maintained on degenerating motoneurons are the boutons colocalized with GAD.

Spinal motoneurons receive a type of cholinergic innervation derived from the C-boutons.^{43,44} C-boutons originate intrinsically from spinal cord neurons,⁸² but the location of these cells remains uncertain. C-boutons could originate from cholinergic interneurons located lateral to the central canal.⁸³ C-boutons identified by vesicular acetylcholine transporter immunoreactivity on spinal motoneurons are lost in autopsy tissue from patients with sporadic ALS.⁸⁴ In G93A-SOD1 mice, vesicular acetylcholine transporter immunoreactivity appeared reduced in the pre-symptomatic phase at day 80 of life,⁶⁷ but our quantitative analysis of ChAT-positive boutons did not show a significant reduction until end-stage disease.

Thus the early loss of boutons on the cell bodies and proximal dendrites of spinal motoneurons in ALS mice seems specific for the glycinergic systems. Changes that may occur more distally in the dendrites of motoneurons await further analysis.

The degeneration of motoneurons seen in G93A-SOD1 mice closely resembles a prolonged necrotic-like process involving early-occurring mitochondrial damage, cellular swelling, and dissolution.³³ Electron microscopy has revealed that mitochondria in the G1H mice acquire DNA damage and swell early and profoundly.^{33,47} Mitochondrial microvacuolar damage seen ultrastructurally in motoneurons emerges by 4 weeks of age in G93A-SOD1 mice with high expression.^{33,47} Mitochondria might be sites of primary toxicity for human mutant SOD1 or the mitochondrial damage is due to some underlying excitotoxic process involving intracellular calcium dysregulation.⁸⁵ We confirmed, using MnSOD-immunoreactivity to mark mitochondria, that mitochondrial swelling is a sign of disease in motoneurons. The onset of prominent mitochondrial swelling seen by confocal microscopy occurs at around 10 weeks of age in G93A-SOD1 mice and escalates rapidly. Our data thus reveal that deficient glycinergic innervation of motoneurons in G93A-SOD1 mice precedes the appearance of major structural pathology in their mitochondria and favors the theory that motoneurons in ALS undergo an excitotoxic process that could be driven partly by loss of inhibitory synaptic modulation.

Glycinergic synapses on spinal motoneurons arise primarily from spinal sources and brain stem.^{86,87} One source of glycinergic innervation of spinal motoneurons is the Renshaw cell.^{55,88} We identified these cells in ALS mouse spinal cord with a calbindin antibody and found that their number is decreased. This is in consistent with the electrophysiological finding that recurrent inhibition was decreased in ALS patients.⁸⁹ The decrease in GlyT2-boutons occurs before the loss of calbindin interneurons, suggesting that the axonal arbors of the Renshaw cell degenerate before the cell body. The loss of Renshaw cells in G93A-SOD1 mice is at least one cellular basis for decreased inhibitory synapses on motoneurons. Loss of putative spinal interneurons has been seen in postmortem human ALS spinal cord^{90,91} and in transgenic mice expressing a mouse mutant SOD1.⁹² Subsets of Renshaw cells and other interneurons in spinal cord, such as parvalbumin-containing neurons, might be at particular risk in ALS mice because they are active metabolically,⁹³ and thus liable to sustain high oxidative stress, and are likely to sustain large intracellular calcium fluxes arising from high-frequency bursting.⁵⁴ It is known that, at least in hippocampus, the parvalbumin-containing interneuron is the most active neuron.^{94,95} The loss of parvalbumin immunopositive neurons, which possibly are GABAergic or glycinergic spinal interneurons,⁹⁶ and α -synuclein-NOS positive interneurons occurs before the loss of motoneurons in ALS mice.³³ It is interesting in this context that somatostatin/NPY GABAergic interneurons in hippocampus appear vulnerable to degeneration before major amyloid deposition in the APP/PSI transgenic mouse model of Alzheimer's disease.⁹⁷ The Renshaw cell

has a critical steady-state role in governing the activity of α -motoneurons and preventing tetanus. The electrophysiological behavior of Renshaw cells is characterized by very high frequency discharge in response to motoneuron recurrent axon collateral excitatory input.⁵⁴ Because mutant SOD1 appears to acquire a toxic property related to oxidative stress and mitochondrial dysfunction,³³ specific subsets of interneurons in spinal cord might be primary sites for pathogenesis in ALS.

In considering this deficient glycinergic innervation of spinal cord motoneurons in ALS mice, it is important to remember the complexity of fine-tuned synaptic communication between excitatory and inhibitory synapses.¹⁹ Loss of glycinergic innervation is likely to be one of the mechanisms that lead to motoneuron hyperexcitability. In conclusion, selective loss of inhibitory glycinergic interneuron regulation of motoneuron function or glycinergic interneuron degeneration could contribute to motoneuron degeneration in ALS. It remains to be determined if interneuronal loss is due to pathology intrinsic to the interneuron or if it is secondary to very early primary disease in their target motoneurons.

Acknowledgments

We thank Ms. Ann Price for the technical assistance.

References

- Rowland LP, Shneider NA: Amyotrophic lateral sclerosis. *N Engl J Med* 2001, 344:1688–1700
- Cleveland DW, Rothstein JD: From Charcot to Lou Gehrig: deciphering selective motor neuron death in ALS. *Nat Rev Neurosci* 2001, 2:806–819
- Rosen DR, Siddique T, Patterson D, Figlewicz DA, Sapp P, Hentati A, Donaldson D, Goto J, O'Regan JP, Deng HX, Rahman Z, Krizus A, McKenna-Yasek D, Cayabyab A, Gaston SM, Berger R, Tanzi RE, Halperin JJ, Herzfeldt B, Van Den Bergh R, Hung W-Y, Bird T, Deng G, Mulder DW, Smyth C, Laing NG, Soriano E, Pericak-Vance MA, Haines J, Rouleau GA, Gusella JS, Horvitz HR, Brown RH: Mutations in Cu/Zn superoxide dismutase gene are associated with familial amyotrophic lateral sclerosis. *Nature* 1993, 362:59–62
- Gurney ME, Pu H, Chiu AY, Dal Canto MC, Polchow CY, Alexander DD, Caliendo J, Hentati A, Kwon YW, Deng HX, Chen W, Zhai P, Sifit RL, Siddique T: Motor neuron degeneration in mice that express a human Cu,Zn superoxide dismutase mutation. *Science* 1994, 264:1772–1775
- Bruijn LI, Miller TM, Cleveland DW: Unraveling the mechanisms involved in motor neuron degeneration in ALS. *Annu Rev Neurosci* 2004, 27:723–749
- Boillee S, Vande Velde C, Cleveland DW: ALS: a disease of motor neurons and their nonneuronal neighbors. *Neuron* 2006, 52:39–59
- Plaitakis A: Glutamate dysfunction and selective motor neuron degeneration in amyotrophic lateral sclerosis: a hypothesis. *Ann Neurol* 1990, 28:3–8
- Rothstein JD, Martin LJ, Kuncl RW: Decreased glutamate transport by the brain and spinal cord in amyotrophic lateral sclerosis. *N Engl J Med* 1992, 326:1464–1468
- Heath PR, Shaw PJ: Update on the glutamatergic neurotransmitter system and the role of excitotoxicity in amyotrophic lateral sclerosis. *Muscle Nerve* 2002, 26:438–458
- Kawahara Y, Kwak S, Sun H, Ito K, Hashida H, Aizawa H, Jeong SY, Kanazawa I: Human spinal motoneurons express low relative abundance of GluR2 mRNA: an implication for excitotoxicity in ALS. *J Neurochem* 2003, 85:680–689
- Kawahara Y, Ito K, Sun H, Aizawa H, Kanazawa I, Kwak S: Glutamate receptors: rRNA editing and death of motor neurons. *Nature* 2004, 427:801
- Zhao P, Ignacio S, Beattie EC, Abood ME: Altered presymptomatic AMPA and cannabinoid receptor trafficking in motor neurons of ALS model mice: implications for excitotoxicity. *Eur J Neurosci* 2008, 27:572–579
- Pieri M, Gaetti C, Spalloni A, Cavalcanti S, Mercuri N, Bernardi G, Longone P, Zona C: alpha-Amino-3-hydroxy-5-methyl-isoxazole-4-propionate receptors in spinal cord motor neurons are altered in transgenic mice overexpressing human Cu,Zn superoxide dismutase (Gly93->Ala) mutation. *Neuroscience* 2003, 122:47–58
- Tortarolo M, Grignaschi G, Calvaresi N, Zennaro E, Spaltro G, Colovic M, Fracasso C, Guiso G, Elger B, Schneider H, Seilheimer B, Caccia S, Bendotti C: Glutamate AMPA receptors change in motor neurons of SOD1G93A transgenic mice and their inhibition by a noncompetitive antagonist ameliorates the progression of amyotrophic lateral sclerosis-like disease. *J Neurosci Res* 2006, 83:134–146
- Eisen A, Weber M: Neurophysiological evaluation of cortical function in the early diagnosis of ALS. *Amyotroph Lateral Scler Other Motor Neuron Disord* 2000, 1 Suppl 1:S47–S51
- Kuo JJ, Schonewille M, Siddique T, Schults AN, Fu R, Bar PR, Anelli R, Heckman CJ, Kroese AB: Hyperexcitability of cultured spinal motoneurons from presymptomatic ALS mice. *J Neurophysiol* 2004, 91:571–575
- Pieri M, Albo F, Gaetti C, Spalloni A, Bengtson CP, Longone P, Cavalcanti S, Zona C: Altered excitability of motor neurons in a transgenic mouse model of familial amyotrophic lateral sclerosis. *Neurosci Lett* 2003, 351:153–156
- Avossa D, Grandolfo M, Mazzarol F, Zatta M, Ballerini L: Early signs of motoneuron vulnerability in a disease model system: characterization of transverse slice cultures of spinal cord isolated from embryonic ALS mice. *Neuroscience* 2006, 138:1179–1194
- Reklung JC, Funk GD, Bayliss DA, Dong XW, Feldman JL: Synaptic control of motoneuronal excitability. *Physiol Rev* 2000, 80:767–852
- Niebroj-Dobosz I, Janik P: Amino acids acting as transmitters in amyotrophic lateral sclerosis (ALS). *Acta Neurol Scand* 1999, 100:6–11
- Malessa S, Leigh PN, Bertel O, Sluga E, Hornykiewicz O: Amyotrophic lateral sclerosis: glutamate dehydrogenase and transmitter amino acids in the spinal cord. *J Neurol Neurosurg Psychiatry* 1991, 54:984–988
- Hayashi H, Suga M, Satake M, Tsubaki T: Reduced glycine receptor in the spinal cord in amyotrophic lateral sclerosis. *Ann Neurol* 1981, 9:292–294
- Whitehouse PJ, Wamsley JK, Zarbin MA, Price DL, Tourtellotte WW, Kuhar MJ: Amyotrophic lateral sclerosis: alterations in neurotransmitter receptors. *Ann Neurol* 1983, 14:8–16
- Mohammadi B, Krampfl K, Moschref H, Dengler R, Bufler J: Interaction of the neuroprotective drug riluzole with GABA(A) and glycine receptor channels. *Eur J Pharmacol* 2001, 415:135–140
- He Y, Benz A, Fu T, Wang M, Covey DF, Zorumski CF, Mennerick S: Neuroprotective agent riluzole potentiates postsynaptic GABA(A) receptor function. *Neuropharmacology* 2002, 42:199–209
- Malgouris C, Bardot F, Daniel M, Pellis F, Rataud J, Uzan A, Blanchard JC, Laduron PM: Riluzole, a novel antigitamate, prevents memory loss and hippocampal neuronal damage in ischemic gerbils. *J Neurosci* 1989, 9:3720–3727
- Eckenstein F, Thoenen H: Production of specific antisera and monoclonal antibodies to choline acetyltransferase: characterization and use for identification of cholinergic neurons. *EMBO J* 1982, 1:363–368
- Arvidsson U, Ulfhake B, Cullheim S, Ramirez V, Shupliakov O, Hokfelt T: Distribution of calbindin D28k-like immunoreactivity (LI) in the monkey ventral horn: do Renshaw cells contain calbindin D28k-LI? *J Neurosci* 1992, 12:718–728
- Antal M, Freund TF, Polgar E: Calcium-binding proteins, parvalbumin and calbindin-D 28k-immunoreactive neurons in the rat spinal cord and dorsal root ganglia: a light and electron microscopic study. *J Comp Neurol* 1990, 295:467–484
- Sanna PP, Celio MR, Bloom FE, Rende M: Presumptive Renshaw cells contain decreased calbindin during recovery from sciatic nerve lesions. *Proc Natl Acad Sci USA* 1993, 90:3048–3052
- Carr PA, Alvarez FJ, Leman EA, Fyffe RE: Calbindin D28k expression in immunohistochemically identified Renshaw cells. *Neuroreport* 1998, 9:2657–2661

32. Alvarez FJ, Dewey DE, Harrington DA, Fyffe RE: Cell-type specific organization of glycine receptor clusters in the mammalian spinal cord. *J Comp Neurol* 1997, 379:150–170
33. Martin LJ, Liu Z, Chen K, Price AC, Pan Y, Swaby JA, Golden WC: Motor neuron degeneration in amyotrophic lateral sclerosis mutant superoxide dismutase-1 transgenic mice: mechanisms of mitochondrialopathy and cell death. *J Comp Neurol* 2007, 500:20–46
34. Poyatos I, Ponce J, Aragon C, Gimenez C, Zafrá F: The glycine transporter GLYT2 is a reliable marker for glycine-immunoreactive neurons. *Brain Res Mol Brain Res* 1997, 49:63–70
35. Spike RC, Watt C, Zafrá F, Todd AJ: An ultrastructural study of the glycine transporter GLYT2 and its association with glycine in the superficial laminae of the rat spinal dorsal horn. *Neuroscience* 1997, 77:543–551
36. Zafrá F, Gomeza J, Olivares L, Aragon C, Gimenez C: Regional distribution and developmental variation of the glycine transporters GLYT1 and GLYT2 in the rat CNS. *Eur J Neurosci* 1995, 7:1342–1352
37. Benowitz LI, Routtenberg A: GAP-43: an intrinsic determinant of neuronal development and plasticity. *Trends Neurosci* 1997, 20:84–91
38. Gorgels TG, Oestreicher AB, de Kort EJ, Gispen WH: Immunocytochemical distribution of the protein kinase C substrate B-50 (GAP43) in developing rat pyramidal tract. *Neurosci Lett* 1987, 83:59–64
39. Skene JH: Axonal growth-associated proteins. *Annu Rev Neurosci* 1989, 12:127–156
40. Skene JH, Jacobson RD, Snipes GJ, McGuire CB, Norden JJ, Freeman JA: A protein induced during nerve growth (GAP-43) is a major component of growth-cone membranes. *Science* 1986, 233:783–786
41. Kalil K, Skene JH: Elevated synthesis of an axonally transported protein correlates with axon outgrowth in normal and injured pyramidal tracts. *J Neurosci* 1986, 6:2563–2570
42. Mackie M, Hughes DI, Maxwell DJ, Tillakaratne NJ, Todd AJ: Distribution and colocalisation of glutamate decarboxylase isoforms in the rat spinal cord. *Neuroscience* 2003, 119:461–472
43. Nagy JI, Yamamoto T, Jordan LM: Evidence for the cholinergic nature of C-terminals associated with subsurface cisterns in alpha-motoneurons of rat. *Synapse* 1993, 15:17–32
44. Li W, Ochalski PA, Brimijoin S, Jordan LM, Nagy JI: C-terminals on motoneurons: electron microscope localization of cholinergic markers in adult rats and antibody-induced depletion in neonates. *Neuroscience* 1995, 65:879–891
45. Navone F, Jahn R, Di Gioia G, Stukenbrok H, Greengard P, De Camilli P: Protein p38: an integral membrane protein specific for small vesicles of neurons and neuroendocrine cells. *J Cell Biol* 1986, 103:2511–2527
46. Purves D, Williams SM: *Neuroscience*. Sunderland, Mass: Sinauer Associates, 2001, xviii, pp. 616, 625, 681, 683
47. Bendotti C, Calvaresi N, Chiveri L, Prella A, Moggio M, Braga M, Silani V, De Biasi S: Early vacuolization and mitochondrial damage in motor neurons of FALS mice are not associated with apoptosis or with changes in cytochrome oxidase histochemical reactivity. *J Neurol Sci* 2001, 191:25–33
48. Higgins CM, Jung C, Xu Z: ALS-associated mutant SOD1G93A causes mitochondrial vacuolation by expansion of the intermembrane space and by involvement of SOD1 aggregation and peroxisomes. *BMC Neurosci* 2003, 4:16
49. Sasaki S, Warita H, Murakami T, Abe K, Iwata M: Ultrastructural study of mitochondria in the spinal cord of transgenic mice with a G93A mutant SOD1 gene. *Acta Neuropathol* 2004, 107:461–474
50. Dal Canto MC, Gurney ME: Development of central nervous system pathology in a murine transgenic model of human amyotrophic lateral sclerosis. *Am J Pathol* 1994, 145:1271–1279
51. Wong PC, Pardo CA, Borchelt DR, Lee MK, Copeland NG, Jenkins NA, Sisodia SS, Cleveland DW, Price DL: An adverse property of a familial ALS-linked SOD1 mutation causes motor neuron disease characterized by vacuolar degeneration of mitochondria. *Neuron* 1995, 14:1105–1116
52. Kong J, Xu Z: Massive mitochondrial degeneration in motor neurons triggers the onset of amyotrophic lateral sclerosis in mice expressing a mutant SOD1. *J Neurosci* 1998, 18:3241–3250
53. Weisiger RA, Fridovich I: Mitochondrial superoxide simutase. Site of synthesis and intramitochondrial localization. *J Biol Chem* 1973, 248:4793–4796
54. Eccles JC, Fatt P, Koketsu K: Cholinergic and inhibitory synapses in a pathway from motor-axon collaterals to motoneurons. *J Physiol* 1954, 126:524–562
55. Curtis DR, Game CJ, Lodge D, McCulloch RM: A pharmacological study of Renshaw cell inhibition. *J Physiol* 1976, 258:227–242
56. Cullheim S, Kellerth JO: Two kinds of recurrent inhibition of cat spinal alpha-motoneurons as differentiated pharmacologically. *J Physiol* 1981, 312:209–224
57. Geiman EJ, Knox MC, Alvarez FJ: Postnatal maturation of gephyrin/glycine receptor clusters on developing Renshaw cells. *J Comp Neurol* 2000, 426:130–142
58. Jursky F, Nelson N: Localization of glycine neurotransmitter transporter (GLYT2) reveals correlation with the distribution of glycine receptor. *J Neurochem* 1995, 64:1026–1033
59. Luque JM, Nelson N, Richards JG: Cellular expression of glycine transporter 2 messenger RNA exclusively in rat hindbrain and spinal cord. *Neuroscience* 1995, 64:525–535
60. Zafrá F, Aragon C, Olivares L, Danbolt NC, Gimenez C, Storm-Mathisen J: Glycine transporters are differentially expressed among CNS cells. *J Neurosci* 1995, 15:3952–3969
61. Roux MJ, Supplisson S: Neuronal and glial glycine transporters have different stoichiometries. *Neuron* 2000, 25:373–383
62. Gomeza J, Ohno K, Hulsman S, Armsen W, Eulenburg V, Richter DW, Laube B, Betz H: Deletion of the mouse glycine transporter 2 results in a hyperekplexia phenotype and postnatal lethality. *Neuron* 2003, 40:797–806
63. Erlander MG, Tillakaratne NJ, Feldblum S, Patel N, Tobin AJ: Two genes encode distinct glutamate decarboxylases. *Neuron* 1991, 7:91–100
64. Kaufman DL, Houser CR, Tobin AJ: Two forms of the gamma-aminobutyric acid synthetic enzyme glutamate decarboxylase have distinct intraneuronal distributions and cofactor interactions. *J Neurochem* 1991, 56:720–723
65. Martin DL, Rimvall K: Regulation of gamma-aminobutyric acid synthesis in the brain. *J Neurochem* 1993, 60:395–407
66. Zang DW, Lopes EC, Cheema SS: Loss of synaptophysin-positive boutons on lumbar motor neurons innervating the medial gastrocnemius muscle of the SOD1G93A G1H transgenic mouse model of ALS. *J Neurosci Res* 2005, 79:694–699
67. Schutz B: Imbalanced excitatory to inhibitory synaptic input precedes motor neuron degeneration in an animal model of amyotrophic lateral sclerosis. *Neurobiol Dis* 2005, 20:131–140
68. Ikemoto A, Kawanami T, Llena JF, Hirano A: Immunocytochemical studies on synaptophysin in the anterior horn of lower motor neuron disease. *J Neuropathol Exp Neurol* 1994, 53:196–201
69. Ikemoto A, Nakamura S, Akiguchi I, Hirano A: Differential expression between synaptic vesicle proteins and presynaptic plasma membrane proteins in the anterior horn of amyotrophic lateral sclerosis. *Acta Neuropathol* 2002, 103:179–187
70. Matsumoto S, Goto S, Kusaka H, Ito H, Imai T: Synaptic pathology of spinal anterior horn cells in amyotrophic lateral sclerosis: an immunohistochemical study. *J Neurol Sci* 1994, 125:180–185
71. Sasaki S, Maruyama S: Decreased synaptophysin immunoreactivity of the anterior horns in motor neuron disease. *Acta Neuropathol* 1994, 87:125–128
72. Schiffer D, Cordera S, Giordana MT, Attanasio A, Pezzulo T: Synaptic vesicle proteins, synaptophysin and chromogranin A in amyotrophic lateral sclerosis. *J Neurol Sci* 1995, 129 Suppl:68–74
73. Cruz-Sanchez FF, Moral A, Rossi ML, Quinto L, Castejon C, Tolosa E, de Belleruche J: Synaptophysin in spinal anterior horn in aging and ALS: an immunohistological study. *J Neural Transm* 1996, 103:1317–1329
74. Ikemoto A, Hirano A, Akiguchi I: Increased expression of growth-associated protein 43 on the surface of the anterior horn cells in amyotrophic lateral sclerosis. *Acta Neuropathol* 1999, 98:367–373
75. Zanette G, Tamburin S, Manganotti P, Refatti N, Forgiione A, Rizzuto N: Different mechanisms contribute to motor cortex hyperexcitability in amyotrophic lateral sclerosis. *Clin Neurophysiol* 2002, 113:1688–1697
76. Zanette G, Tamburin S, Manganotti P, Refatti N, Forgiione A, Rizzuto N: Changes in motor cortex inhibition over time in patients with amyotrophic lateral sclerosis. *J Neurol* 2002, 249:1723–1728
77. Turner MR, Osei-Lah AD, Hammers A, Al-Chalabi A, Shaw CE, Andersen PM, Brooks DJ, Leigh PN, Mills KR: Abnormal cortical excitability in sporadic but not homozygous D90A SOD1 ALS. *J Neurol Neurosurg Psychiatry* 2005, 76:1279–1285
78. Lloyd CM, Richardson MP, Brooks DJ, Al-Chalabi A, Leigh PN: Ex-

- tramotor involvement in ALS: PET studies with the GABA(A) ligand [(11C)]flumazenil. *Brain* 2000, 123 (Pt 11):2289–2296
79. Petri S, Krampfl K, Hashemi F, Grothe C, Hori A, Dengler R, Bufler J: Distribution of GABAA receptor mRNA in the motor cortex of ALS patients. *J Neuropathol Exp Neurol* 2003, 62:1041–1051
 80. Petri S, Kollwe K, Grothe C, Hori A, Dengler R, Bufler J, Krampfl K: GABA(A)-receptor mRNA expression in the prefrontal and temporal cortex of ALS patients. *J Neurol Sci* 2006, 250:124–132
 81. Petri S, Schmalbach S, Grosskreutz J, Krampfl K, Grothe C, Dengler R, Van Den Bosch L, Robberecht W, Bufler J: The cellular mRNA expression of GABA and glutamate receptors in spinal motor neurons of SOD1 mice. *J Neurol Sci* 2005, 238:25–30
 82. McLaughlin BJ: Propriospinal and supraspinal projections to the motor nuclei in the cat spinal cord. *J Comp Neurol* 1972, 144:475–500
 83. Miles GB, Hartley R, Todd AJ, Brownstone RM: Spinal cholinergic interneurons regulate the excitability of motoneurons during locomotion. *Proc Natl Acad Sci USA* 2007, 104:2448–2453
 84. Nagao M, Misawa H, Kato S, Hirai S: Loss of cholinergic synapses on the spinal motor neurons of amyotrophic lateral sclerosis. *J Neuropathol Exp Neurol* 1998, 57:329–333
 85. Bendotti C, Carri MT: Lessons from models of SOD1-linked familial ALS. *Trends Mol Med* 2004, 10:393–400
 86. Zafra F, Aragon C, Gimenez C: Molecular biology of glycinergic neurotransmission. *Mol Neurobiol* 1997, 14:117–142
 87. Legendre P: The glycinergic inhibitory synapse. *Cell Mol Life Sci* 2001, 58:760–793
 88. Fyffe RE: Glycine-like immunoreactivity in synaptic boutons of identified inhibitory interneurons in the mammalian spinal cord. *Brain Res* 1991, 547:175–179
 89. Raynor EM, Shefner JM: Recurrent inhibition is decreased in patients with amyotrophic lateral sclerosis. *Neurology* 1994, 44:2148–2153
 90. Oyanagi K, Ikuta F, Horikawa Y: Evidence for sequential degeneration of the neurons in the intermediate zone of the spinal cord in amyotrophic lateral sclerosis: a topographic and quantitative investigation. *Acta Neuropathol* 1989, 77:343–349
 91. Stephens B, Guilloff RJ, Navarrete R, Newman P, Nikhar N, Lewis P: Widespread loss of neuronal populations in the spinal ventral horn in sporadic motor neuron disease. A morphometric study. *J Neurol Sci* 2006, 244:41–58
 92. Morrison BM, Janssen WG, Gordon JW, Morrison JH: Time course of neuropathology in the spinal cord of G86R superoxide dismutase transgenic mice. *J Comp Neurol* 1998, 391:64–77
 93. Carr PA, Liu M, Zaruba RA: Enzyme histochemical profile of immunohistochemically identified Renshaw cells in rat lumbar spinal cord. *Brain Res Bull* 2001, 54:669–674
 94. Pawelzik H, Hughes DI, Thomson AM: Physiological and morphological diversity of immunocytochemically defined parvalbumin- and cholecystokinin-positive interneurons in CA1 of the adult rat hippocampus. *J Comp Neurol* 2002, 443:346–367
 95. Klausberger T, Magill PJ, Marton LF, Roberts JD, Cobden PM, Buzsaki G, Somogyi P: Brain-state- and cell-type-specific firing of hippocampal interneurons in vivo. *Nature* 2003, 421:844–848
 96. Alvarez FJ, Jonas PC, Sapir T, Hartley R, Berrocal MC, Geiman EJ, Todd AJ, Goulding M: Postnatal phenotype and localization of spinal cord V1 derived interneurons. *J Comp Neurol* 2005, 493:177–192
 97. Ramos B, Baglietto-Vargas D, del Rio JC, Moreno-Gonzalez I, Santa-Maria C, Jimenez S, Caballero C, Lopez-Tellez JF, Khan ZU, Ruano D, Gutierrez A, Vitorica J: Early neuropathology of somatostatin/NPY GABAergic cells in the hippocampus of a PS1xAPP transgenic model of Alzheimer's disease. *Neurobiol Aging* 2006, 27:1658–1672